Journal of Process Control 44 (2016) 14–22

Contents lists available at ScienceDirect

Journal of Process Control

journal homepage: www.elsevier.com/locate/jprocont

Closed-loop growth-rate regulation in fed-batch dual-substrate processes with additive kinetics based on biomass concentration measurement

Sebastián Nuñez*, Fabricio Garelli, Hernán De Battista

Grupo de Control Aplicado (GCA), Instituto LEICI, UNLP-CONICET, Facultad de Ingeniería, Universidad Nacional de La Plata, Argentina

ARTICLE INFO

Article history:
Received 25 August 2015
Received in revised form 1 April 2016
Accepted 6 May 2016
Available online 26 May 2016

Keywords:
Growth rate regulation
Dual-substrate
Fed-batch process
Non-linear control

ABSTRACT

This paper deals with the design of feeding rates for dual-substrate fed-batch processes where the main control objective is the regulation of the microbial growth rate. To this end, feedback of the growth rate error is incorporated to a biomass proportional dual feeding law. A second-order sliding mode observer is used to estimate the growth rate, so that no additional sensors are required. Stability conditions are derived and robustness against several disturbances such as yield uncertainty, measurement errors and kinetic model mismatch is analytically and numerically evaluated. The advantages of the proposal include: minimal measurement requirements, regulation with fast convergence to the desired growth rate and reduced regulation error in the presence of disturbances.

1. Introduction

Biotechnological processes are applied for the production of metabolites required in the food, pharmaceutical and chemical industries. They also have application in alternative energy generation including production of hydrogen, butane and methane from renewable resources, in the development of new products such as bio-polymers [1], and in remediation of toxic substances such as benzene, phenol and toluene [2,3].

Currently, there exists an increasing interest for multiple-feed processes. These cultures can be considered for enhancing metabolites production [4] and increasing degradation efficiency of toxic compounds [5]. In a multi-substrate process, microbial growth rate is influenced by two or more substrates. These nutrients may perform the same function within the cells, as in the case of two carbon sources, or may be used to fulfil different nutritional requirements, as in the case of a carbon and a nitrogen source [6]. Different types of growth kinetic models have been developed to describe the microbial behavior including additive growth, multiplicative growth, growth in two phases (diauxic growth) and enhanced growth due to a second metabolic pathway [6,7]. From an unstructured point of view, these kinetics lead to different non-linear expressions for the specific growth rate (μ) and the specific rates of substrates consumption.

Fed-batch processes are often preferred to batch ones when maximizing cell or product formation is pursued but chemical reactions are inhibited by some substrate in excess. Also they are a suitable option when some kinetic rate needs to be controlled. In many applications, growth rate regulation is a primary goal since this key variable is closely related to the metabolic state of the microorganism [8]. In fact, controlling growth rate is relevant to avoid formation of undesired by-products when maximizing production of heterologous proteins [9] and to guarantee reproducibility between fed-batch cultivations [10]. Particularly for dual-substrate processes, an additional control objective is to regulate the growth on each of the substrates. This requirement follows, for example, from the relation between substrate consumption and desired product properties [11]. In other cases, feeding of a second nutrient to be degraded or a cheaper carbon source is considered.

With the aim of providing multiple nutrients to the bioreactor, a number of open-loop feeding strategies have been proposed. Many of these strategies are extensions of the feeding laws used in processes with only one-limiting substrate [12,13]. In [14], independent glycerol and methanol exponential feeding rates were designed for increasing productivity of the process. In [5], a dual-exponential feeding law is considered, where the second substrate is fed to increase biodegradation of phenol. In more advanced approaches, the feeding flow rates are adjusted on-line as function of measured variables. In [15], the feeding flow rates increase in proportion to biomass, thus reducing problems associated with nutrient underfeeding or overfeeding. However, since there is no closed-loop w.r.t. growth rate, modelling errors may degrade

* Corresponding author.
E-mail address: sebastian.nuniez@ing.unlp.edu.ar (S. Nuñez).

http://dx.doi.org/10.1016/j.jprocont.2016.05.003
0959-1524/

regulation. Then, in [16] a non-linear feeding law was proposed based on the assumption that the individual growth rates are known or can be estimated separately. The fact of distinguishing the growth rates on each substrate may require measurement of more than one substance concentration, for example biomass and one of the substrates.

This paper considers a bioreactor fed with two substrates where the main objective is regulating the growth rate to a given set-point μ_{ref}, which is assumed to be compatible with a desired physiological state of the micro-organism. This set-point is calculated to achieve an specific objective, e.g. to avoid by-products formation, to optimize biodegradation [5], to maintain a metabolic state [10] or to increase the volumetric productivity of a metabolite [14]. The proposed strategy deals with processes that exhibit additive growth kinetics and can be used for supplying two carbon sources. The control law is inspired on closed-loop feeding laws for μ regulation in one-limiting substrate processes [17]. So, the biomass proportional dual feeding rate of previous works is preserved [15,16], but now the proportionality gains are continuously adjusted as function of the total growth rate error. Since there exist growth rate observers based on biomass concentration measurement, already required to implement the biomass proportional feeding strategy, no additional sensors are required for implementing the closed-loop scheme.

The rest of the paper is organized as follows. In Section 2, the model of the fed-batch process is described and the closed loop dual-substrate feeding law is presented. In Section 3, convergence properties are analyzed for different additive kinetics and robustness analysis is performed. In Section 4, the proposed strategy is evaluated under nominal and uncertain conditions. Concluding remarks are given in Section 5.

2. Feeding flow rate design

2.1. Dual-substrate model and control objective

Microbial growth in a fed-batch process under well-mixed condition can be described with the following mass balance model [18]

$$\dot{x} = \mu x - \frac{x}{v}F_1 - \frac{x}{v}F_2, \tag{1a}$$

$$\dot{s}_1 = -\sigma_1 x + \frac{(S_{1in} - s_1)}{v}F_1 - \frac{s_1}{v}F_2, \tag{1b}$$

$$\dot{s}_2 = -\sigma_2 x - \frac{s_2}{v}F_1 + \frac{(S_{2in} - s_2)}{v}F_2, \tag{1c}$$

$$\dot{v} = F_1 + F_2, \tag{1d}$$

where x, s_1 and s_2 are concentration of biomass and substrates (g/L) and v is the working volume. The specific growth rate is given by $\mu(s_1, s_2)$ and the substrate consumption rates are denoted by σ_1 and σ_2. The control inputs are the feeding flow rates of each substrate (F_i) where the inlet concentrations are denoted by $S_{(i)in}$. In this paper, additive growth rate is considered, so the total μ is the sum of two non-negative terms

$$\mu = \mu_1 + \mu_2. \tag{2}$$

The substrate consumption rates can be represented as

$$\sigma_i = \mu_i / y_i, \tag{3}$$

with $y_i > 0$ being the yield of substrate i to biomass.

In this work, it is considered that the primary goal of the feeding applied to the dual-substrate process (1) is the regulation of the growth rate while maintaining a given ratio between substrates s_1/s_2 or between the individual growth rates μ_1/μ_2. That is, it is desired to regulate μ at $\mu_{ref} = \mu_{1r} + \mu_{2r}$, where μ_{ir} stands for the desired growth rate value on substrate i. Therefore, the nominal trajectory for biomass is an exponential profile where the biomass $X(t) = xv$ evolves as

$$X^*(t) = x_0 v_0 e^{\mu_{ref} t}, \tag{4}$$

where x_0, v_0 stand for the initial values of biomass concentration and volume, respectively. Furthermore, it can be observed that:

1. Biomass concentration follows a bounded trajectory given by the logistic function

$$x^*(t) = \frac{\mu_{ref}/\lambda_r}{1 + \left(\frac{\mu_{ref}}{\lambda_r x_0} - 1\right) e^{-\mu_{ref} t}}, \tag{5}$$

   with $\lambda_r = \lambda_{1r} + \lambda_{2r}$ being constant gains to be determined later.
2. Volume grows unbounded.
3. Substrate concentrations are constant at (s_{1r}, s_{2r}) for which the desired growth rates (μ_{1r}, μ_{2r}) are obtained.

Growing at constant rate requires feeding the reactor in proportion to biomass population. If biomass and volume measurements are available, flow rates proportional to biomass

$$F_i = \lambda_{ir} x v, \tag{6}$$

can be applied. The proper proportionality gains λ_{ir} can be determined by making the substrate dynamics invariant at s_{ir} after replacing F_i in Eqs. (1b) and (1c) with Eq. (6):

$$\dot{s}_1 = \left(-\frac{\mu_{1r}}{y_1} + (S_{1in} - s_{1r})\lambda_{1r} - s_{1r}\lambda_{2r}\right) x = 0, \tag{7a}$$

$$\dot{s}_2 = \left(-\frac{\mu_{2r}}{y_2} + (S_{2in} - s_{2r})\lambda_{2r} - s_{2r}\lambda_{1r}\right) x = 0, \tag{7b}$$

Since $x(t) \geq \underline{x} > 0$, the solution follows from the linear equations

$$\begin{pmatrix} S_{1in} - s_{1r} & -s_{1r} \\ -s_{2r} & S_{2in} - s_{2r} \end{pmatrix} \begin{pmatrix} \lambda_{1r} \\ \lambda_{2r} \end{pmatrix} = \begin{pmatrix} \frac{\mu_{1r}}{y_1} \\ \frac{\mu_{2r}}{y_2} \end{pmatrix}, \tag{8}$$

and the result is [15]

$$\lambda_{1r} = \frac{\frac{\mu_{1r}}{y_1}(S_{2in} - s_{2r}) + \frac{\mu_{2r}}{y_2}s_{1r}}{S_{1in}S_{2in} - S_{2in}s_{1r} - S_{1in}s_{2r}}, \tag{9a}$$

$$\lambda_{2r} = \frac{\frac{\mu_{2r}}{y_2}(S_{1in} - s_{1r}) + \frac{\mu_{1r}}{y_1}s_{2r}}{S_{1in}S_{2in} - S_{2in}s_{1r} - S_{1in}s_{2r}}. \tag{9b}$$

2.2. Dual feeding law with feedback of the growth rate

The application of the feeding law (6) with gains defined in (9) stabilizes the substrate concentrations at (s_{1r}, s_{2r}). Indeed, global stability is achieved for monotonic kinetics while, naturally, only local stability can be guaranteed when multiplicity occurs due to substrate inhibition. This can be shown with the help of a quadratic Lyapunov function and partial stability theory [15]. The main shortcomings of this control strategy are that convergence speed is very low and steady state errors caused by model uncertainties are high.

In order to speed up convergence and reduce regulation errors due to model uncertainties, closed loop control of the growth rate must be implemented. We propose here to shape the proportionality gains as function of the error in μ regulation as follows

$$F_i = \lambda_{ir}(1 + f_\mu(e))xv. \tag{10}$$

where

$$e = \mu_{ref} - \mu \tag{11}$$

and $f_\mu(e)$ is an increasing function satisfying $f_\mu(0)=0$. Since the input flow rates are non-negative, a necessary constraint for the feedback function is $f_\mu(\cdot)>-1$. A key advantage of the proposed feedback structure is that global stability results, similar to those obtained for (6), can be reached as shown later. From the practical viewpoint, the proposed feedback law can be implemented without extra measurement requirements. In fact, the on-line value of μ used to construct the feedback function (Eq. (10)) can be obtained from the same biomass and volume measurements used for implementing (6) by means of a μ observer (i.e. a software sensor). In particular, a second-order sliding-mode observer developed in [19] by the authors is employed and is briefly described in Section 4, although other observers can alternatively be used. The main advantage of this observer is its finite time convergence, so it does not extend the order of the dynamical system.

3. Stability and robustness features of the proposed control

3.1. Closed loop dynamics

Recall that the control law is designed to stabilize the substrate concentrations at s_{ir} in order to accomplish the regulation objective. In fact, if substrate concentrations go to (s_{1r}, s_{2r}), then biomass concentration will follow a trajectory of the form (5) whereas the culture volume will grow exponentially until the end of the cultivation. It will be shown next that, thanks to the feedback structure of the proposed control law, stability features can be determined by just studying the substrate dynamics. After replacing the feeding rates F_i in Eqs. (1b) and (1c) with Eq. (10), the substrate dynamics result in

$$\dot{s}_i = -z_i x + (S_{(i)in}\lambda_{ir} - s_i\lambda_r)f_\mu x, \tag{12}$$

with

$$z_i \triangleq \mu_i/y_i - (S_{(i)in}\lambda_{ir} - s_i\lambda_r) = \frac{\mu_i - \mu_{ir}}{y_i} + \lambda_r(s_i - s_{ir}), \tag{13a}$$

$$\lambda_r \triangleq \lambda_{1r} + \lambda_{2r}. \tag{13b}$$

Since biomass concentration is always positive and bounded, the change of time scale $\dot{s}_i = s_i' x$ can be applied, yielding

$$s_i' = -z_i + (S_{(i)in}\lambda_{ir} - s_i\lambda_r)f_\mu = f_{si}. \tag{14}$$

Note that the substrate dynamics (14) in the new time scale do not depend on biomass and volume. Thus, stability properties of the feedback controller can be determined by studying the autonomous second order dynamical system of substrates concentration. This is the advantage of preserving the biomass proportional flow rates in the feedback strategy (10).

3.2. Global stability features: the monotonic case

We will derive next global stability conditions for the dual substrate feedback control law, which are similar to those obtained for the control (6). In this case, obtaining a Lyapunov function for the nonlinear second-order substrate dynamics is not trivial. Consequently, a different approach comprising three steps is followed here: (i) check if there exists an invariant region $\mathcal{R}$, so that every trajectory starting in or entering $\mathcal{R}$ stays in $\mathcal{R}$, (ii) check if (s_{1r}, s_{2r}) is the only equilibrium point in $\mathcal{R}$ for the dynamics (14) and (iii) check if there are no closed orbits in $\mathcal{R}$. If all these steps are fulfilled, then all trajectories of (s_1, s_2) evolve towards the desired operating point (s_{1r}, s_{2r}). General stability results for monotonic kinetics are presented here. How inhibition and interaction in the growth kinetics affect stability is discussed later.

Consider for the moment kinetics of the form:

$$\mu(s_1, s_2) = \mu_1(s_1) + \mu_2(s_2) \tag{15a}$$

$$\mu_i(0) = 0 \tag{15b}$$

$$\frac{\partial \mu_i}{\partial s_i} > 0, \quad \forall s_i \in [0, S_{(i)in}] \tag{15c}$$

Substrates concentrations have physical meaning in the subset $\mathcal{S} = \{(s_1, s_2) \in \mathbb{R}^2 : 0 \le s_1 \le S_{1in}, 0 \le s_2 \le S_{2in}\}$. We define a region $\mathcal{R} \subset \mathcal{S}$ given by

$$\mathcal{R} = \left\{(s_1, s_2) \in \mathcal{S} : s_1 \le S_{1in}\frac{\lambda_{1r}}{\lambda_r}, s_2 \le S_{2in}\frac{\lambda_{2r}}{\lambda_r}\right\}. \tag{16}$$

From Eq. (14), it can be shown that s_i' evaluated at $s_i^\star = S_{(i)in}(\lambda_{ir}/\lambda_r)$ (with $s_j \ge 0, j \ne i$) results in $s_i' = -\mu_i/y_i < 0$. Then, substrate trajectories evaluated on these boundaries point inwards $\mathcal{R}$. Similarly, $s_i' \le -\mu_i/y_i < 0$ for $s_i > s_i^\star$. The same argument can be used at the boundaries defined by $s_i = 0$, where the dynamics are:

$$s_i' = S_{(i)in}\lambda_{ir}(1 + f_\mu(e)) > 0. \tag{17}$$

Thus, it can be concluded that substrate trajectories entering or starting in $\mathcal{R}$ do not leave this subset.

Fig. 1 shows the line $\mu = \mu_{ref}$ (i.e. $e=0$) typical for monotonic kinetics on the invariant region $\mathcal{R}$. Region $\mathcal{R}$ is divided into four subsets by the lines $z_i = 0$. Note that, for monotonic kinetics of the form (15), $s_i = s_{ir}$ on each of these lines. Then, the intersection of these lines is the desired equilibrium point (s_{1r}, s_{2r}). It will be shown now that, for monotonic kinetics of the form (15), there is no other equilibrium point in $\mathcal{R}$. In region A it is verified that $e>0$ and so $f_\mu > 0$, whereas both $z_i = ((\mu_i - \mu_{ir})/y_i) + \lambda_r(s_i - s_{ir}) < 0$. Therefore, both $s_i' > 0$ in region A, and no equilibrium points exist there. The same reasoning can be used to conclude that there are not equilibrium points in region B where $f_\mu < 0$ and both $z_i = ((\mu_i - \mu_{ir})/y_i) + \lambda_r(s_i - s_{ir}) > 0$. In region C, $z_1 > 0$ whereas $z_2 < 0$, so there cannot exist f_μ that simultaneously cancel both substrate dynamics. An analogous result is obtained for region D. Finally, on the lines $s_i = s_{ir}$, the substrate dynamics reduce to $s_i' = (S_{(i)in}\lambda_{ir} - s_i\lambda_r)f_\mu$ that is cancelled only at $f_\mu = 0$, that is at the intersection between both lines that is the desired equilibrium point.

Finally, the absence of closed orbits in $\mathcal{R}$ can be shown by applying the Bendixson's Criterion [20]. From Eq. (14) it can be written

$$\begin{pmatrix} s_1' \\ s_2' \end{pmatrix} = \boldsymbol{f} = \begin{pmatrix} f_{s1} \\ f_{s2} \end{pmatrix}, \tag{18}$$

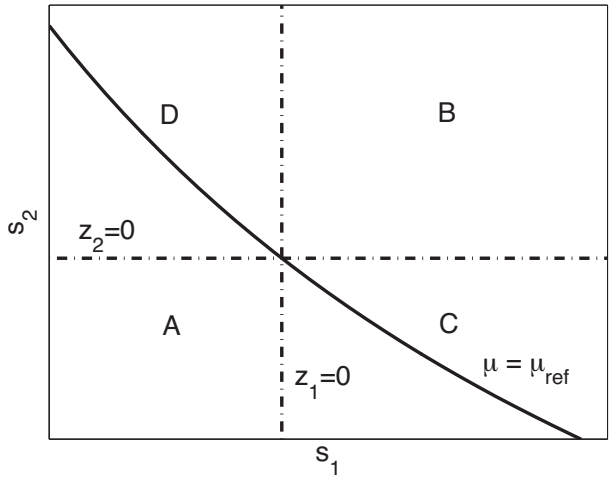

Fig. 1. Analysis of convergence of feeding law (10): regions defined on the subset $\mathcal{S}$ for analysis of equilibrium points.

and the divergence of (18) results

$$\nabla \boldsymbol{f} = \frac{\partial f_{s1}}{\partial s_1} + \frac{\partial f_{s2}}{\partial s_2}. \tag{19}$$

By differentiating (14) w.r.t. s_i, each term of the previous Eq. is given by

$$\frac{\partial f_{si}}{\partial s_i} = -\frac{\partial z_i}{\partial s_i} - \lambda_r f_\mu + \frac{\partial f_\mu}{\partial s_i}(S_{(i)in}\lambda_{ir} - s_i\lambda_r), \tag{20}$$

with

$$\frac{\partial z_i}{\partial s_i} = \frac{1}{y_i}\frac{\partial \mu_i}{\partial s_i} + \lambda_r, \tag{21a}$$

$$\frac{\partial f_\mu}{\partial s_i} = \frac{\partial f_\mu}{\partial e}\frac{\partial e}{\partial s_i} = -\frac{\partial f_\mu}{\partial e}\frac{\partial \mu}{\partial s_i}. \tag{21b}$$

Then, by replacing Eqs. (20) and (21) in (19), the divergence results in

$$\nabla \boldsymbol{f} = -\left(\frac{1}{y_1}\frac{\partial \mu_1}{\partial s_1} + \frac{1}{y_2}\frac{\partial \mu_2}{\partial s_2}\right) - 2\lambda_r(1+f_\mu) - \frac{\partial f_\mu}{\partial e}\left(\frac{\partial \mu}{\partial s_1}(S_{1in}\lambda_{1r} - s_1\lambda_r) + \frac{\partial \mu}{\partial s_2}(S_{2in}\lambda_{2r} - s_2\lambda_r)\right). \tag{22}$$

Since the feedback function f_μ was designed so that $1+f_\mu(e)>0$ and $(\partial f_\mu/\partial e)\geq 0$ for all e, it follows that $\nabla \boldsymbol{f}<0$ in (at least) region $\mathcal{R}$ for any additive monotonic kinetics of the form (15). Consequently, as $\nabla \boldsymbol{f}$ is not identically zero and does not change sign, there are no closed orbits in $\mathcal{R}$ (Theorem 2.7, p. 42 in [20]).

Finally, as all state trajectories initiated in $\mathcal{S}$ enter and stay in a region where there are not closed orbits and only one equilibrium point exists, then that equilibrium point is globally stable. Note that this is a general result valid for all dual monotonic kinetics. The simplest example of this type of kinetics combines two Monod ones:

$$\mu = \sum_{i=1}^{2} \frac{\mu_{\max i} s_i}{k_{si} + s_i} \tag{23}$$

but other monotonic kinetic models such as Blackman or Luong can be combined.

3.3. Discussion: stability features for other additive kinetics

In the following sections, the effect of substrate interaction and inhibition on the stability features of the proposed control law will be discussed.

3.3.1. Kinetics with substrate interaction

In many processes, growth rate is governed by monotonic kinetics but there are some interaction or competitiveness between substrates. So, more general expressions for the growth kinetics can be considered:

$$\mu(s_1, s_2) = \mu_1(s_1, s_2) + \mu_2(s_1, s_2) \tag{24a}$$

$$\mu_1(0, \cdot) = \mu_2(\cdot, 0) = 0 \tag{24b}$$

$$\frac{\partial \mu_i}{\partial s_i} > 0, \qquad \frac{\partial \mu_i}{\partial s_j} \neq 0, \quad \forall s_i \in [0, S_{(i)in}], \quad j \neq i \tag{24c}$$

The reasoning made before to conclude that all trajectories of substrate dynamics enter and stay on $\mathcal{R}$ is still valid. The uniqueness of the operating point (s_{1r}, s_{2r}) can be determined following a similar reasoning as before. Finally, since $\partial \mu_j/\partial s_{i\neq j}$ may be negative, then $\partial \mu/\partial s_i = \partial \mu_i/\partial s_i + \partial \mu_j/\partial s_i$ may also be negative in certain regions of $\mathcal{R}$. Consequently, general results about definite negativeness of the divergence (22) cannot be stated. However, if the interaction is not strong enough to change the sign of $\nabla \boldsymbol{f}$, then non-existence of closed orbits can be guaranteed and global stability can still be achieved in consequence. This must be checked for each particular process.

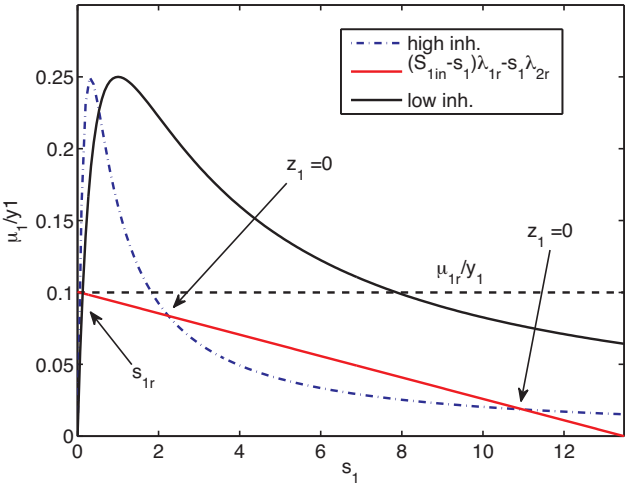

Fig. 2. Analysis of kinetics with substrate inhibition.

A typical example of this type of kinetics with interaction is

$$\mu = \sum_{i=1}^{2} \frac{\mu_{\max i} s_i}{s_i + k_{si} + I_i s_j}, \quad j \neq i \tag{25}$$

where the larger coefficients I_i, the stronger the interaction between substrates is. This function is widely used for modelling processes including biodegradation of toxic compounds [2].

3.3.2. Non-monotonic kinetics

In many other processes with additive kinetics, at least one of the terms, say $\mu_1(s_1)$, exhibits inhibition at high substrate concentrations. That is, μ_1 is maximum at a substrate concentration $s_{\max 1} \in (0, S_{1in})$. So, $\partial \mu_1/\partial s_1$ becomes negative for $s_1 > s_{\max 1}$.

Even though $\mu_1(s_1) = \mu_{1r}$ may have two solutions s_{1r} and $s_1^* > s_{1r}$, s_{1r} may still be the only stationary solution provided inhibition is low enough. This is illustrated in Fig. 2 where two different kinetic functions (scaled by the yield y_1) are plotted. In the case of low inhibition (solid line), the kinetic function intersects the line $S_{1in}\lambda_{1r} - s_1\lambda_r = 0$ only at s_{1r}. So, it can be stated following the same reasoning as for monotonic kinetics that (s_{1r}, s_{2r}) is the only equilibrium point. Again, general results about definite negativeness of the divergence (22) cannot be stated because $(\partial \mu_1/\partial s_1) < 0$ for high values of s_1. If inhibition is low enough, $\nabla \boldsymbol{f}$ will be negative all along $\mathcal{R}$ and closed orbits will not exist. Then, global stability can still be guaranteed for that particular process.

Conversely, if inhibition is too strong, the straight line in Fig. 2 intersects the kinetic function more than once (see μ_1/y_1 (dashed line)). Note that z_1 changes its sign at each intersection point. Therefore multiple equilibria may appear. In that case, as it is obvious, just local stability can be achieved.

A typical example of this type of kinetics combines a Haldane kinetics that exhibits a maximum at $s_{\max 1} = \sqrt{k_{s1}k_{i1}}$ with a Monod one:

$$\mu = \frac{\mu_{o1} s_1}{s_1 + k_{s1} + s_1^2/k_{i1}} + \frac{\mu_{\max 2} s_2}{s_2 + k_{s2}}. \tag{26}$$

3.4. Robustness features

One of the main sources of uncertainty for the calculation of exponential feeding of fed-batch reactors in both open- and

closed-loop operation is the uncertainty in the substrate-to-biomass yields. Variations in the yields usually appear because of incomplete modelling of the chemical reactions taking place along the process. Hence the importance of determining how the proposed feedback control improves the regulation features. Uncertainties in the kinetic functions introduce regulation errors through the gains λ_{ir} that can also be reduced by feedback. However, since sensitivity to kinetics uncertainty is much lower than to yield, it is ignored in this analysis for the sake of brevity.

On the other hand, as the proposed control law uses biomass concentration and volume measurements to implement both the feeding law proportional to cell population and the feedback action, it is also important to determine how measurement errors affect regulation. It will be shown that feedback also reduces regulation errors caused by sensor deviations.

3.4.1. Robustness against yield uncertainty

From Eqs. (13a)–(14), it follows that in equilibrium ($s_i' = 0$)

$$\mu_{ir} = (S_{(i)in}\lambda_{ir} - \lambda_r s_{ir})y_i. \tag{27}$$

If now the yields are perturbed by δy_i, then the stationary values of s_i and μ_i move to satisfy

$$\delta\mu_i + \mu_{ir} = (S_{(i)in}\lambda_{ir} - \lambda_r(\delta s_i + s_{ir}))(y_i + \delta y_i)(1 + f(-\delta\mu_i - \delta\mu_j)). \tag{28}$$

Assuming small deviations from the nominal conditions, the deviation from the equilibrium point can be approximated by

$$\delta\mu_i \approx \mu_{ir}\frac{\delta y_i}{y_i} - \lambda_r y_i \delta s_i + \mu_{ir} f(-\delta\mu_i - \delta\mu_j). \tag{29}$$

Calling $m_i = \left.\frac{\partial\mu_i}{\partial s_i}\right|_{s=s_{ir}}$ and $k_f = \left.\frac{\partial f}{\partial e}\right|_{e=0}$, the linearization of Eq. (29) yields

$$\begin{pmatrix} a_1 + k_f & k_f \\ k_f & a_2 + k_f \end{pmatrix}\begin{pmatrix}\delta\mu_1 \\ \delta\mu_2\end{pmatrix} \approx \begin{pmatrix}\frac{\delta y_1}{y_1} \\ \frac{\delta y_2}{y_2}\end{pmatrix} \tag{30}$$

where $a_i = (1 + \lambda_r y_i/m_i)/\mu_{ir}$. Then the errors in the individual growth rates μ_i result, approximately

$$\begin{pmatrix}\delta\mu_1 \\ \delta\mu_2\end{pmatrix} \approx \frac{\begin{pmatrix} a_2 + k_f & -k_f \\ -k_f & a_1 + k_f\end{pmatrix}}{a_1a_2 + k_f(a_1 + a_2)}\begin{pmatrix}\frac{\delta y_1}{y_1} \\ \frac{\delta y_2}{y_2}\end{pmatrix}. \tag{31}$$

Note that the feedback of the total growth rate couples both channel errors, that is the uncertainty in y_i produces an error in both μ_i and μ_j. Summing these individual terms, the steady state error in the total growth rate regulation is, approx.,

$$\delta\mu \approx \frac{a_1^{-1}\frac{\delta y_1}{y_1} + a_2^{-1}\frac{\delta y_2}{y_2}}{1 + k_f(a_1^{-1} + a_2^{-1})}. \tag{32}$$

It is clear how the linearized growth rate feedback gain k_f reduces the total growth rate error in comparison to the baseline control (6) where (32) holds for $k_f = 0$.

Expression (32) can be further simplified if a_i is approximated by $a_i = 1/\mu_{ir}$ as usually happens in reality. Effectively, in that case

$$\frac{\delta\mu}{\mu_{ref}} \approx \frac{\frac{\mu_{1r}}{\mu_{ref}}\frac{\delta y_1}{y_1} + \frac{\mu_{2r}}{\mu_{ref}}\frac{\delta y_2}{y_2}}{1 + k_f\mu_{ref}}. \tag{33}$$

3.4.2. Robustness against biomass sensor deviations

Next, it will be determined how biomass sensor errors affect regulation. The main causes of error depend on the sensor used, but typically are wrong calibration and nonlinearities in the sensor response. The error in biomass sensor not only produces an error in the dilution, but also in the estimation of the growth rate to be fed back in the controller:

$$x_m = x + \delta x, \tag{34a}$$

$$F_i = \lambda_{ir}x_m v(1 + f_\mu(\mu_{ref} - \widehat{\mu})), \tag{34b}$$

$$D = \frac{F_1 + F_2}{v}, \tag{34c}$$

where x_m is the measured value, δx is the measurement error and D is the dilution.

Propagation of errors introduced by volume sensors can be determined in a similar fashion, so it will not be treated here.

Observers typically include a state, say $\widehat{x}$, that tracks the measured biomass concentration signal. In sliding mode and high gain observers $\widehat{x}$ copies x. Then, it can be said that $\dot{\widehat{x}} = \dot{x}$. So, ideally, the estimated growth rate tracks the real growth rate signal. However, when measurement error is introduced, an estimation error $\widetilde{\mu} = \widehat{\mu} - \mu$ appears:

$$\dot{\widehat{x}} = \left(\widehat{\mu} - \frac{F_1 + F_2}{v}\right)x_m = \left(\mu - \frac{F_1 + F_2}{v}\right)x = \dot{x}. \tag{35}$$

Then, it follows that

$$\widetilde{\mu} \approx -(\mu - D)\delta x/x \tag{36}$$

where second order terms were neglected. Recall that during μ regulation substrate keeps constant while biomass follows the logistic curve (5), i.e. $s_i = s_{ir}$ and $(\mu - D) = \mu_{ref} - \lambda_r x^*(t)$. Then, equalling to zero the substrates dynamics (1b) and (1c) with feeding flows (10) perturbed by δx and $\widetilde{\mu}$ yields

$$\dot{s}_i = -\frac{\mu_i}{y_i}x + (S_{(i)in}\lambda_{ir} - \lambda_r s_i)(x + \delta x)(1 + f_\mu(\mu_{ref} - \mu - \widetilde{\mu})) = 0. \tag{37}$$

Then, assuming small deviations from the set-point, and using a_i and k_f defined before, the growth rate deviations are the solutions of:

$$\begin{pmatrix} a_1 + k_f & k_f \\ k_f & a_2 + k_f\end{pmatrix}\begin{pmatrix}\delta\mu_1 \\ \delta\mu_2\end{pmatrix} \approx \begin{pmatrix}1 \\ 1\end{pmatrix}(1 + k_f\mu_{ref} - k_f\lambda_r x^*)\frac{\delta_x}{x^*}. \tag{38}$$

That is,

$$\delta\mu = \left(\frac{a_1 + a_2}{a_1a_2 + k_f(a_1 + a_2)}\right)(1 + k_f\mu_{ref} - k_f\lambda_r x^*)\frac{\delta_x}{x^*}. \tag{39}$$

If a_i is approximated by $a_i = 1/\mu_{ir}$ as before, a simplified version is found

$$\frac{\delta\mu}{\mu_{ref}} \approx \left[1 - \frac{k_f\lambda_r x^*}{1 + k_f\mu_{ref}}\right]\frac{\delta_x}{x^*}. \tag{40}$$

Note that $x^*(t)$ evolves from $x(0)$ to $x_{\max} = \mu_{ref}/\lambda_r$. Thus, the factor in brackets is always greater than zero and lower than one. This means that the regulation error introduced by biomass measurement deviations is reduced with feedback. Moreover, at the end of the process it is reduced by a factor $(1 + k_f\mu_{ref})$.

4. Numerical assessment and discussion

In this section, the proposed feeding law is evaluated under nominal conditions, several kinetic models and uncertainties. All

results are compared with those obtained using the baseline controller (6). The biomass measurement used to implement the proposed and baseline controllers is corrupted with ±0.1 g/L additive noise weighted in the range of 2–10 h^{-1}. This bandwidth was selected to evaluate the effects of low frequency noise in the closed loop performance.

The feedback function f_μ in Eq. (10) used here is

$$f_\mu(e) = \max(k_f e, -1), \tag{41}$$

with $k_f = 10$. This simple function provides linear gain around $\mu = \mu_{ref}$ and avoids negative flow rates. It is worth noting that other lower-bounded functions can alternatively be used.

4.1. Growth rate estimation

The required estimate of the specific growth rate can be obtained from observers. Biomass based observers are particularly suited since biomass measurement is already required for determining the flow rates. Among several options, sliding mode algorithms provide finite-time convergence despite non-linearities and disturbances. In this application we consider the μ-observer presented in [19]:

$$\dot{\widehat{x}} = (-D + \widehat{\mu} + 2\overline{\rho}\beta|\sigma|^{1/2} sign(\sigma))\widehat{x}, \tag{42a}$$

$$\dot{\widehat{\mu}} = \overline{\rho}\alpha\, sign(\sigma), \tag{42b}$$

$$\sigma = 1/\overline{\rho}\, \log(x_m/\widehat{x}), \tag{42c}$$

where $\widehat{x}$ is estimated biomass concentration and $\widehat{\mu}$ is the estimated growth rate, σ is the sliding surface which is based on the natural logarithm of $x_m/\widehat{x}$ and $\overline{\rho}$ is an upper bound for $|\dot{\mu}|$. With suitable tuning of α and β, the observer reaches $\widetilde{x} = x_m - \widehat{x} = 0$ in finite-time and a continuous estimate of μ is achieved. The importance of the finite-time convergence is that no additional dynamics is added by the observer, hence the stability of the closed loop is not threatened. In this application the observer parameters were $\overline{\rho} = 0.5$, $\alpha = 1.1$, $\beta = 0.9$. The parameter $\overline{\rho}$ is typically obtained from experience on the process. Tuning of parameters α, β and a discussion on the selection of $\overline{\rho}$ can be found in [19]. In the simulations, initial conditions for observer states were $\widehat{x}(0) = x(0) > 0$ g/L (i.e. the first measured value is considered) and $\widehat{\mu}(0) = 0.2\,h^{-1}$. It is worth noting that other algorithms with finite-time convergence can alternatively be used for the implementation of the closed-loop feeding laws [21,22].

4.2. Results for monotonic kinetics under nominal condition

Results are presented first for a dual Monod kinetic model as in Eq. (23) where the parameters are listed in Table 1. These results show the improvement in the transient response obtained with the proposed feedback law w.r.t. the baseline controller. To illustrate the transient, the set-point switches after 10 h from $\mu_{refA} = 0.20\,h^{-1}$ to $\mu_{refB} = 0.1\,h^{-1}$, while keeping the ratio between individual growth rates at $\mu_{1r}/\mu_{2r} = 1$ all along the process.

Fig. 3a shows the time evolution of μ_1, μ_2 and the total growth rate μ. The closed-loop of μ was activated at $t_{on} = 0.50\,h^{-1}$

Table 1
Numerical values used in Section 4.

Process parameters and initial conditions			
μ_{max1}	0.5 h^{-1}	μ_{max2}	0.2 h^{-1}
k_{s1}	0.5 g/L	k_{s2}	0.5 g/L
y_1	2 g/g	y_2	2.1 g/g
S_{1in}	20 g/L	S_{2in}	20 g/L
$x(0)$	5 g/L	$v(0)$	1 L
$s_1(0)$	0.03 g/L	$s_2(0)$	0.05 g/L
Operating point 1: $\mu_{refA} = 0.20\,h^{-1}$			
μ_{1r}	0.10 h^{-1}	s_{1r}	0.125 g/L
μ_{2r}	0.10 h^{-1}	s_{2r}	0.50 g/L
Operating point 2: $\mu_{refB} = 0.10\,h^{-1}$			
μ_{1r}	0.05 h^{-1}	s_{1r}	0.05 g/L
μ_{2r}	0.05 h^{-1}	s_{2r}	0.16 g/L

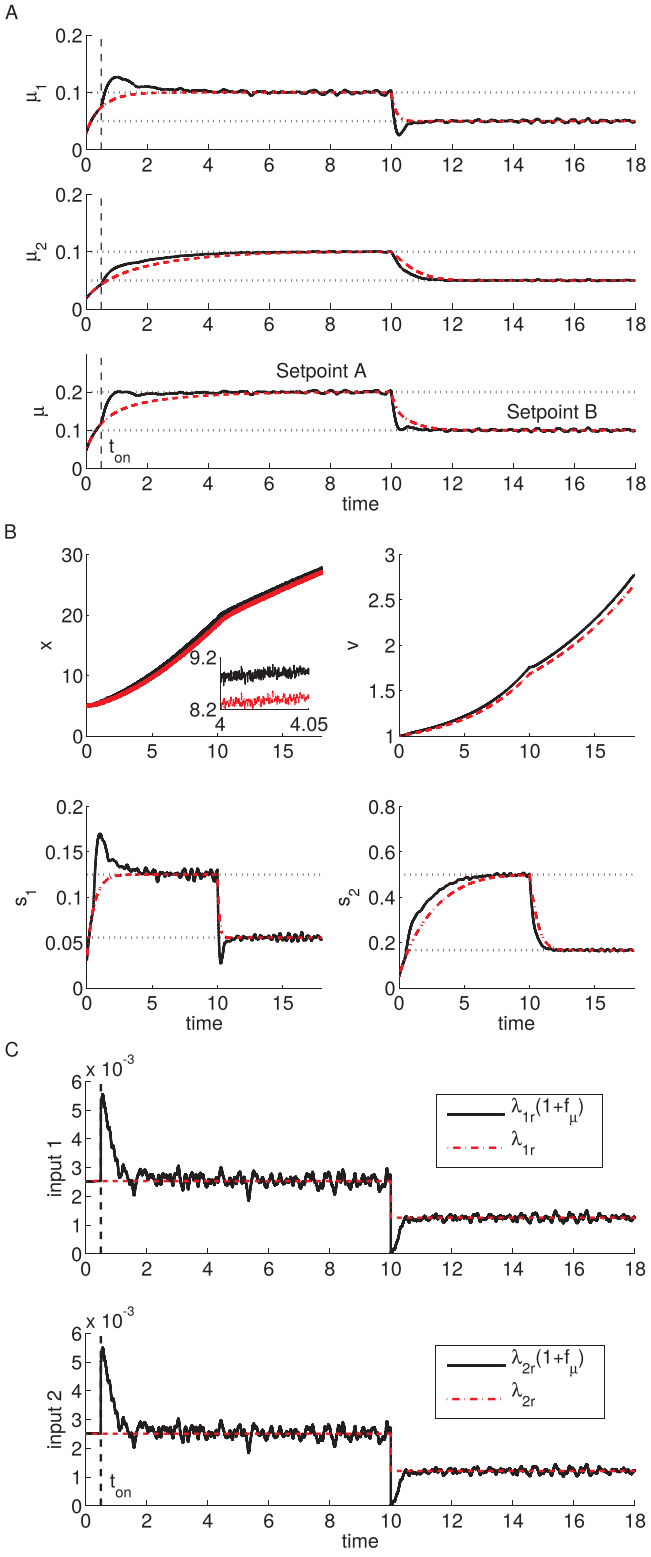

Fig. 3. Results under nominal conditions using the proposed feedback control (black solid lines) and the baseline control (red dashed lines). (A) Specific growth rates; (B) states; (C) feeding flow gains. (For interpretation of the references to color in this figure legend, the reader is referred to the web version of this article.)

after observer convergence (42). The results of μ regulation are compared with those obtained with the baseline control (6). The proposed feedback (10)–(41) exhibits a substantial reduction of convergence time from 4 to approx. 1 h. The time evolution of the states is presented in Fig. 3b, where it is seen the evolution of the substrates concentration towards the values (s_{1r}, s_{2r}) for both set-points. The substrate responses are also plotted on the $s_1 - s_2$ plane in Fig. 4. Fig. 3c shows the gains applied to each input, where it is seen the effect of the feedback term on the first 2 h of cultivation due to the error in μ. As described previously, the closed-loop response can be further improved by increasing the feedback gain k_f in (41). Of course, a trade-off arises when tuning k_f between fastening the transient response and noise amplification.

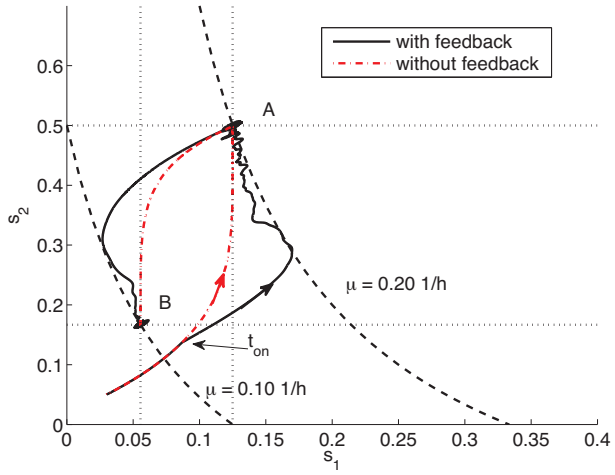

Fig. 4. Results under nominal conditions. Evolution of substrate concentrations on the plane $(s_1 - s_2)$.

4.3. Results for other kinetics

In this case, interaction between substrates is considered. The kinetic model (25) was used to run the process, where the interactive parameters I_i were chosen as $I_1 = k_{s1}/k_{s2}$, $I_2 = 1/I_1$ to represent competitive inhibition effect. Since this competitiveness is ignored when computing the substrate stationary values s_{ir}, this kinetic model is also a source of uncertainty. Fig. 5a shows the time profile of the growth rates, where it is seen that the biomass-proportional laws (6) and (10) were able to regulate this process with substrate interaction. In particular, the feedback controller led to faster convergence to both set-points, whereas the steady state error is negligible. This is corroborated in Fig. 5b where the state trajectory for both controllers is plotted on the plane $s_1 - s_2$ together with the surface levels of Eq. (25). It is verified that the baseline controller suffers from a small error almost eliminated by feedback.

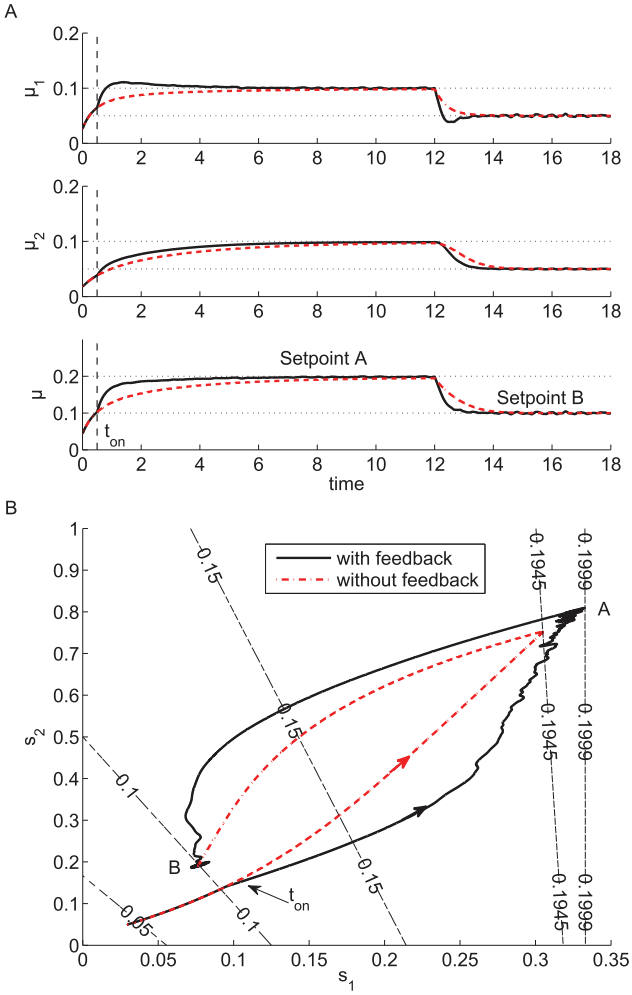

Fig. 5. Results for kinetics with interaction. (A) Specific growth rates; (B) evolution of substrate concentrations on the plane $(s_1 - s_2)$ and surface levels of kinetics (25).

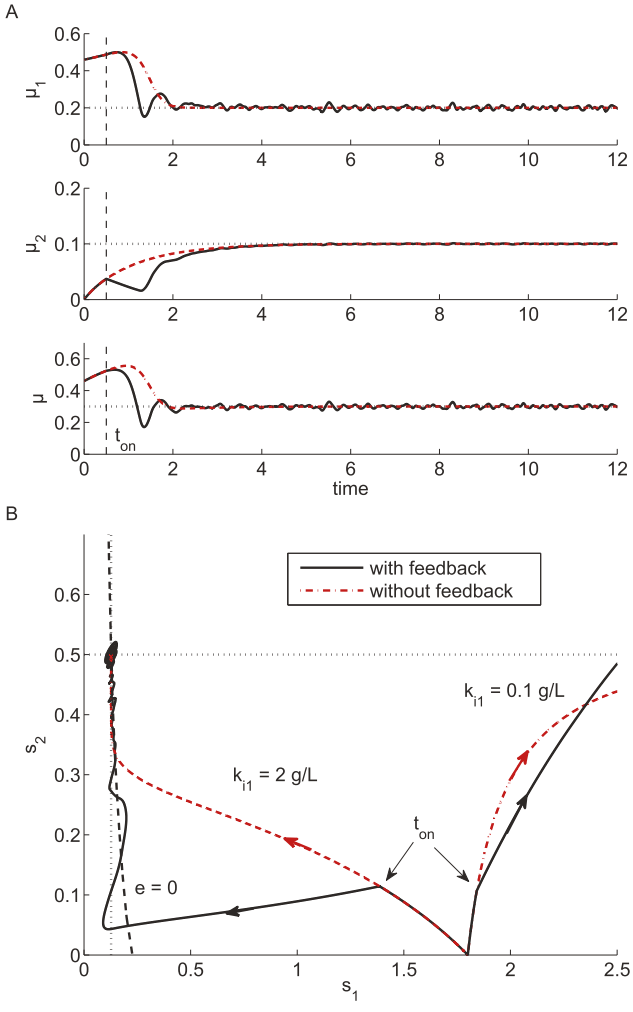

Fig. 6. Results for kinetics with inhibition. (A) Specific growth rates with $k_{i1} = 2$ g/L. (B) Evolution of substrate concentrations on the plane $(s_1 - s_2)$ for $k_{i1} = 2$ g/L and $k_{i1} = 0.1$ g/L.

Fig. 6 shows the result in case one growth rate is a non-monotonic term (Eq. (26)). The parameters $\mu_{o1} = 1\,h^{-1}$ and $k_{i1} = 2$ g/L were considered for μ_1 and the rest of the parameters are the same as in Table 1. The desired set-point is $\mu_{ref} = 0.3\,h^{-1}$ and $\mu_{1r}/\mu_{2r} = 2$. Given that μ_1 has a maximum at $s_{max\,1} = \sqrt{k_{s1}k_{i1}} = 1$ g/L, initial condition $s_1(0) = 1.8$ g/L was selected in order to show convergence from the right-hand side of the maximum, which is critical for stability. Both biomass-proportional feeding laws regulate the growth rate at the desired set-point, but the feedback controller provides faster convergence to the set-point. If higher inhibition is present, multiplicity appears and the process may evolve from certain initial conditions to an undesired operation mode (see trajectories of substrates in Fig. 6b for $k_{i1} = 0.1$ g/L). This type of undesirable response, predicted by the stability analysis performed before, is very well known in bioprocess control and also appears in μ regulation of one-limiting substrate processes with inhibition. Therefore, to regulate safely this type of process, the initial conditions should be low. Limiting the flow rates in a similar fashion as in [17] could be explored to obtain stable responses from everywhere, but the cost to pay will be a loss of performance from low initial conditions.

4.4. Results for yield and measurement errors

In order to evaluate the robustness against yield errors, a 30% overestimation in the substrate-to-biomass yield y_2 was considered. Fig. 7a plots the state trajectories for both controllers on the $s_1 - s_2$ plane, putting in evidence the steady state errors in μ regulation. The regulation error is significant because the yields directly affect the computation of the proportionality gains λ_{ir}. It is clear that the proposed feedback controller (10) reduces the growth rate error in comparison with the baseline controller. The steady state concentrations estimated using the results of Section 3.4.1 are indicated with cross mark symbols. The estimated errors in μ for the given operating point are $\delta\mu \approx -0.021\,h^{-1}$ and $\delta\mu \approx -0.008\,h^{-1}$ for the baseline and feedback controllers, respectively. These values, as well as the steady state substrate concentrations, were determined with the help of Eqs. (31) and (32). To conclude, the proposed feeding law is also effective in reducing the regulation error under yield mismatch.

Another source for errors is wrong calibration of the biomass sensor. Fig. 7b shows the substrates trajectories in case of a −5% error in biomass concentration measurement. Note that the proposed feedback reduces the error in μ, i.e. for both operating points the substrates converge close to the point (s_{1r}, s_{2r}). Thus, as predicted in Eq. (40), the proposed feedback of μ reduces the regulation error under biomass sensor deviations.

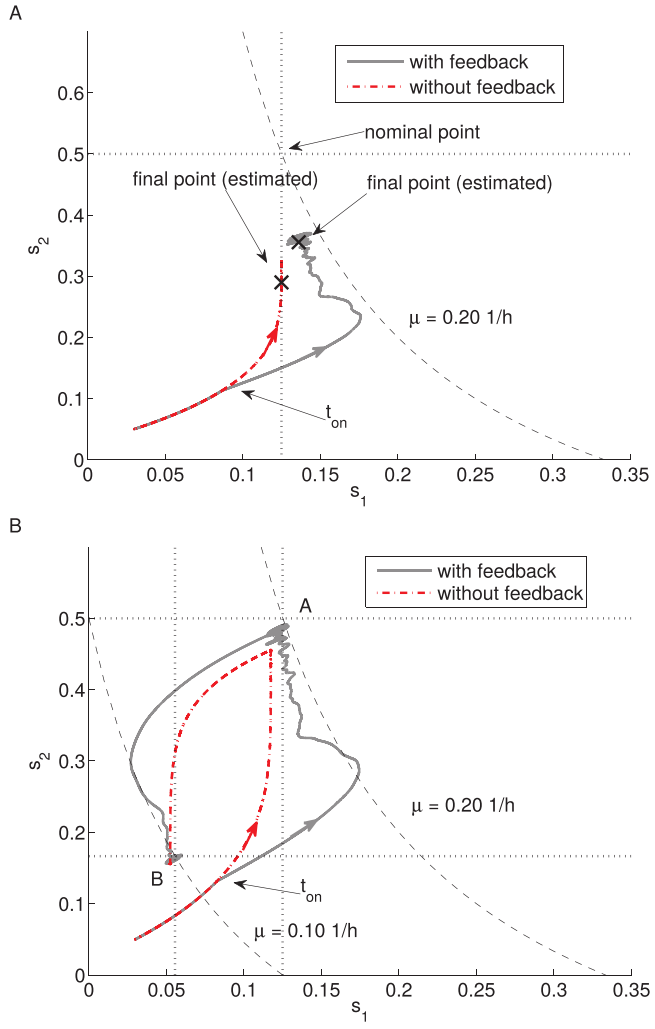

Fig. 7. Results for errors on the plane $(s_1 - s_2)$. (A) Uncertainty in y_2. (B) Biomass measurement error (−5%).

5. Conclusion and future work

Until now, stable control of the specific growth rate in multi-substrate processes was guaranteed without feedback of the regulated variable. Hence, there was no possibility of adjusting the convergence time or mitigating the effect of modelling errors. The application of closed-loop feeding laws proportional to biomass can improve the regulation of the microbial growth rate during the cultivation while preserving the stability properties. This was shown in this work for fed-batch processes with additive growth kinetics. In fact, faster convergence to the desired set-points and better regulation under model uncertainty were obtained. Particularly, modelling mismatching in the form of yield uncertainty, substrate interaction and substrate inhibition were satisfactorily coped by the proposed feedback controller. Similarly, regulation error caused by sensor offsets were significantly reduced by feedback.

Future work could consider the extension to multiplicative kinetic terms, domains of attraction in case of multiplicity, bounding of the flow rate to avoid unstable responses, integral control actions to eliminate steady-state errors, etc.

Acknowledgments

This work was supported by the Agency for the Promotion of Science and Technology ANPCyT (PICT 2014-2394), the National Research Council CONICET (PIP 112-201501-00837) and Universidad Nacional de La Plata of Argentina.

References

[1] W. Wu, S.-Y. Lai, M.-F. Jang, Y.-S. Chou, Optimal adaptive control schemes for PHB production in fed-batch fermentation of *Ralstonia eutropha*, J. Process Control 23 (2013) 1159–1168.
[2] D.E. Trigueros, A.N. Módenes, A.D. Kroumov, F.R. Espinoza-Quiñones, Modeling of biodegradation process of BTEX compounds: kinetic parameters estimation by using particle swarm global optimizer, Process Biochem. 45 (2010) 1355–1361.
[3] J. Liu, X. Jia, J. Wen, Z. Zhou, Substrate interactions and kinetics study of phenolic compounds biodegradation by *Pseudomonas* sp. cbp 1-3, Biochem. Eng. J. 67 (2012) 156–166.
[4] W.-C. Kao, D.-S. Lin, C.-L. Cheng, B.-Y. Chen, C.-Y. Lin, J.-S. Chang, Enhancing butanol production with *Clostridium pasteurianum* CH4 using sequential glucose–glycerol addition and simultaneous dual-substrate cultivation strategies, Bioresour. Technol. 135 (2013) 324–330.
[5] B.-Y. Chen, J.-W. You, J.-S. Chang, Optimal exponential feeding strategy for dual-substrate biostimulation of phenol degradation using *Cupriavidus taiwanensis*, J. Hazard. Mater. 168 (2009) 507–514.

[6] M. Zinn, B. Witholt, T. Egli, Dual nutrient limited growth: models, experimental observations, and applications, J. Biotechnol. 113 (2004) 263–279.
[7] Z. Soons, J. Voogt, G. van Straten, A. van Boxtel, Constant specific growth rate in fed-batch cultivation of *Bordetella pertussis* using adaptive control, J. Biotechnol. 125 (2006) 252–268.
[8] M.M. Schuler, I. Marison, Real-time monitoring and control of microbial bioprocesses with focus on the specific growth rate: current state and perspectives, Appl. Microbiol. Biotechnol. 94 (2012) 1469–1482.
[9] E. Anane, E. van Rensburg, J.F. Görgens, Optimisation and scale-up of α-glucuronidase production by recombinant *Saccharomyces cerevisiae* in aerobic fed-batch culture with constant growth rate, Biochem. Eng. J. 81 (2013) 1–7.
[10] D.V.R. Neeleman, C. Beuvery, G. van Straten, A. van Boxtel, Dual-substrate feedback control of specific growth-rate in vaccine production, Comput. Appl. Biotechnol. 2004 (2004) 427–432.
[11] J. Xu, B. Guo, Z. Zhang, Q. Wu, Q. Zhou, J. Chen, G. Chen, G. Li, A mathematical model for regulating monomer composition of the microbially synthesized polyhydroxyalkanoate copolymers, Biotechnol. Bioeng. 90 (2005) 821–829.
[12] M.C. d'Anjou, A.J. Daugulis, Mixed-feed exponential feeding for fed-batch culture of recombinant methylotrophic yeast, Biotechnol. Lett. 22 (2000) 341–346.
[13] H. Huang, D. Ridgway, T. Gu, M. Moo-Young, Enhanced amylase production by *Bacillus subtilis* using a dual exponential feeding strategy, Bioprocess Biosyst. Eng. 27 (2004) 63–69.
[14] H. Moon, S. Kim, J. Lee, S. Rhee, E. Choi, H. Kang, I. Kim, S. Hong, Independent exponential feeding of glycerol and methanol for fed-batch culture of recombinant *Hansenula polymorpha* DL-1, Appl. Biochem. Biotechnol. 111 (2003) 65–79.
[15] E. Picó-Marco, J.L. Navarro, A closed-loop exponential feeding law for multi-substrate fermentation processes, in: Proceedings of the 17th IFAC World Congress, 2008, pp. 9685–9689.
[16] A. Vignoni, S. Nuñez, H. De Battista, J. Picó, E. Picó-Marco, F. Garelli, Specific kinetic rates regulation in multi-substrate fermentation processes, in: 12th IFAC Symposium on Computer Applications in Biotechnology, 2013, pp. 42–47.
[17] H. De Battista, J. Picó, E. Picó-Marco, Globally stabilizing control of fed-batch processes with Haldane kinetics using growth rate estimation feedback, J. Process Control 16 (2006) 865–875.
[18] J. Nielsen, J. Villadsen, G. Lidén, Bioreaction Engineering Principles, Kluwer Academic Plenum Publishers, 2003.
[19] H. De Battista, J. Picó, F. Garelli, J.L. Navarro, Reaction rate reconstruction from biomass concentration measurement in bioreactors using modified second-order sliding mode algorithms, Bioprocess Biosyst. Eng. 35 (2012) 1615–1625.
[20] S. Sastry, Planar dynamical systems Nonlinear Systems, vol. 10, Springer, New York, 1999, pp. 31–75.
[21] H. De Battista, J. Picó, F. Garelli, A. Vignoni, Specific growth rate estimation in (fed-)batch bioreactors using second-order sliding observers, J. Process Control 21 (2011) 1049–1055.
[22] A. Vargas, J. Moreno, A. Vande Wouwer, A weighted variable gain super-twisting observer for the estimation of kinetic rates in biological systems, J. Process Control 24 (2014) 957–965.